



# Structure of Computer-Generated Arterial Trees with Different Optimization Target Functions

M. Neumann, W. Schreiner, R. Karch, F. Neumann

*Department of Medical Computer Sciences, Department of Cardiothoracic Surgery, Institute of Experimental Physics, University of Vienna, Spitalgasse 23, A-1090 Vienna, Austria  
E-Mail: friederike.neumann@akh-wien.ac.at*

## Abstract

Highly realistic models of coronary arterial trees can be generated on the computer by our method of “constrained constructive optimization” (CCO). Basic concepts of real arterial trees have been accounted for by the specific choice of boundary conditions, constraints, and target functions for geometrical and structural optimization. By variation of the parameter  $\lambda$  - the spatial dimensionality of the global property being minimized - the structure of the resulting trees changes drastically, which is immediately evident to visual inspection: vessel shape varies from strongly meandering structures through more and more streamlined paths to fully straightened tubes. This gradual change of vessel shapes can be theoretically explained by our particular choice of target functions. Statistically, vessel shape can be characterized by numerical indices such as blood transport path length or relative segment orientation, which change in a typical way with the variation of the optimization parameter.

## 1 Introduction

Sufficient supply of blood to all sites of tissue can be considered as the basic task of arterial vessel trees. Since blood has to be delivered through the arteries to their respective perfusion sites in an efficient way, the question of optimality arises most naturally in this context (cf. Thompson [1]). Experimental studies have been performed to obtain morphometric measurements of arterial segment radii, lengths, and branching angles. Theoretical con-



## 38 Simulations in Biomedicine IV

siderations have shown that several optimization criteria can be formulated which are physiologically reasonable. Minimum intravascular volume of the vessel tree is one of the generally accepted targets for optimization (Kamiya & Togawa [2]). In our CCO model, arterial vessel trees are grown in a stepwise fashion by successively adding new segments; additionally, a target function is chosen whose value must be minimized at each step of tree generation (Schreiner & Buxbaum [3]). In the present study, arterial trees were optimized according to a family of cost (target) functions, parameterized by an exponent  $\lambda$ , which characterizes the spatial dimensionality of the property being minimized. For the specific choice  $\lambda = 2$ , this is equivalent to optimizing for minimum volume. In the following we will show the influence of varying this parameter  $\lambda$  on the structural properties of the resulting trees (cf. Schreiner *et al.* [4]).

## 2 Tree structures in CCO

### 2.1 How the tree is grown

In the present study, the trees were generated within a circular two-dimensional area representing the piece of tissue to be perfused. The terminal segments of each tree were required to be uniformly distributed within this area to perfuse it as homogeneously as possible. The resolution of the trees, as given by the number of terminal segments, was set to  $N_{\text{term}} = 4000$ . For dichotomously branching trees, the total number of segments is always given by  $N_{\text{tot}} = 2N_{\text{term}} - 1$ , regardless of the particular structure of the tree.

CCO trees are grown by successively adding terminal segments at randomly chosen perfusion sites and generating new bifurcations. In accordance with morphometric measurements on corrosion casts of real arterial trees, the radii of parent and daughter segments at each bifurcation were assumed to obey a power law

$$r_{\text{parent}}^{\gamma} = r_{\text{left}}^{\gamma} + r_{\text{right}}^{\gamma}, \quad (1)$$

with typical values of  $\gamma$  falling in the range between 2.5 and 3 (Rodbard [5], Sherman [6]). For all trees of the present work  $\gamma$  was set to 3.0.

In order to perfuse a circular area of radius  $r_{\text{perf}} = 5$  cm under “physiological” conditions, perfusion pressure, terminal pressure, and total perfusion flow were set to  $p_{\text{perf}} = 100$  mm Hg,  $p_{\text{term}} = 60$  mm Hg, and  $Q_{\text{perf}} = 680$  ml/min, respectively, and kept constant in all simulations. After adding a new bifurcation, all segment radii were rescaled according to Poiseuille’s law for laminar flow resistance so that at any time during the growth process, all terminal segments delivered equal flows (i.e., an identical fraction of  $Q_{\text{perf}}$ ) at equal pressures ( $p_{\text{term}}$ ).

Since this can be achieved for arbitrary positions of the new bifurcation within the existing tree, the topological location and the geometry of each bifurcation are optimized by minimizing a cost (or target) function. Suitable

cost functions are defined in terms of the functional structure of the tree and may be derived from global properties of the vascular tree, such as minimum surface or total volume. Our target function was chosen to be of the general form

$$T = \sum_{i=1}^{N_{\text{tot}}} \ell_i r_i^\lambda \rightarrow \min, \quad (2)$$

where  $\ell_i$  and  $r_i$  are length and radius of segment  $i$ . The exponent may take on every real value  $\lambda \geq 0$ . Setting  $\lambda$  equal to 0, 1, 2, 3... is—apart from a multiplicative factor—equivalent to minimizing the sum of segment lengths, total surface, intravasal volume, or “hypervolume”, respectively. Typical geometrical and topological structures of the trees emerge due to the value of  $\lambda$ .

## 2.2 Quantifying tree structures

What is intuitively clear from visual inspection of trees generated with different values of the target function parameter  $\lambda$  of Eq. (2) (cf. Fig. 1), may also be characterized by various numerical indices. The figure shows clearly that different values of  $\lambda$  will primarily affect the length of the path blood has to traverse from the root segment to the site of delivery (terminal segment). With  $\lambda = 0$  a long detour is necessary to deliver blood to a given perfusion site, as compared to trees with  $\lambda > 0$ . This detour of blood flow can, for instance, be described by the number of generations or bifurcation levels ( $n_{\text{bif}}$ ) along its route from the root to the terminal segment. It can also be quantified by the ratio between the actual path length of blood transport to a particular terminal segment

$$L_{\text{path}} = \sum_{i \in \text{path}} \ell_i \quad (3)$$

and the corresponding “bee-line” (a straight line connecting the terminal to the root segment):

$$R_L = L_{\text{path}}/L_{\text{bee-line}}, \quad R_L \geq 1. \quad (4)$$

A different, but related aspect of tree structure is given by the following index of segment orientation, defined as the angle between a segment’s direction and the direction of a straight line from the proximal end of the root segment to the distal end of segment  $i$ ,

$$\varphi_i = \arccos(\mathbf{s}_i \cdot \mathbf{b}_i), \quad (5)$$

where  $\mathbf{s}_i$  and  $\mathbf{b}_i$  are the unit vectors pointing in the direction of the bee-line and the symmetry axis of segment  $i$ . This index characterizes the deviation of the actual direction of blood transport by a given segment from the direction in which blood would be delivered along the shortest path.

## 40 Simulations in Biomedicine IV

Additionally, it can be expected that global quantities, such as sum of segment lengths, total surface, intravascular volume or hypervolume of the tree will change with different values of  $\lambda$  and will be minimized only if they are used as target functions in the optimization process.

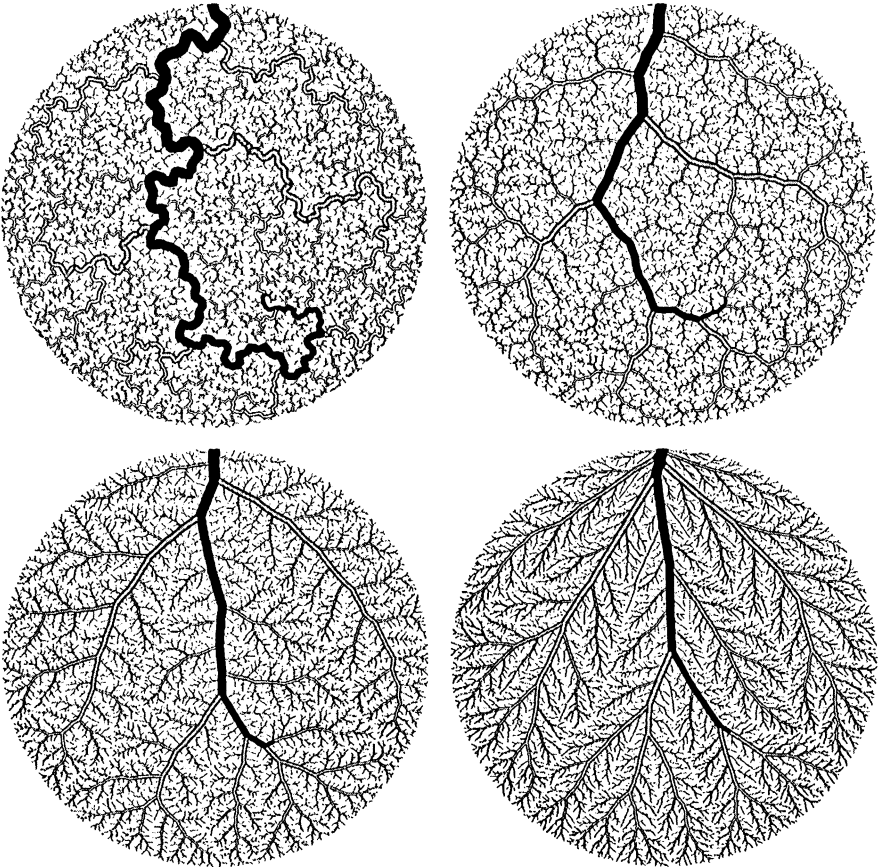


Figure 1: Dependence of tree structure on the parameter of the target function  $\lambda$  [Eq. (2)]. Vessel shapes change drastically when  $\lambda$  is varied from 0 (top left) through 1 and 2 (top right and bottom left) to 3 (bottom right). The path to a specific fixed location within the perfusion area has been marked in all trees.

## 2.3 The target function parameter and tree structures

As mentioned earlier, except for a numerical factor, we recover for  $\lambda = 0, 1, 2, \dots$  in Eq. (2) the sum of segment lengths, total surface, volume or hypervolumes as target functions. On the other hand, each of these quantities can be calculated for *any* CCO tree and may be compared to the value obtained if this quantity *itself* assumes the role of the target function. Figure 2 shows for five trees with  $\lambda = 0, 1, \dots, 4$  the relative size of each quantity normalized to its minimum value. The individual curves show that each quantity takes on its minimum value if—and only if—it is being used as the target function (since it is the object of minimization; filled circles), but increases steadily (i.e., becomes more and more suboptimal) toward both larger and smaller values of  $\lambda$  (open circles). The ratio of the actual value of any quantity to its minimum represents the degree of optimality which can still be achieved for this aspect of functional structure, even when it has not been used as target function. For instance, the intravasal volume of a tree optimized for minimum total surface ( $\lambda = 1$ ) is only 7% larger than that of a tree with minimum volume. On the other hand, optimizing the tree with respect to the sum of segment lengths ( $\lambda = 0$ ) results in a volume as large as 240% of the minimum value.

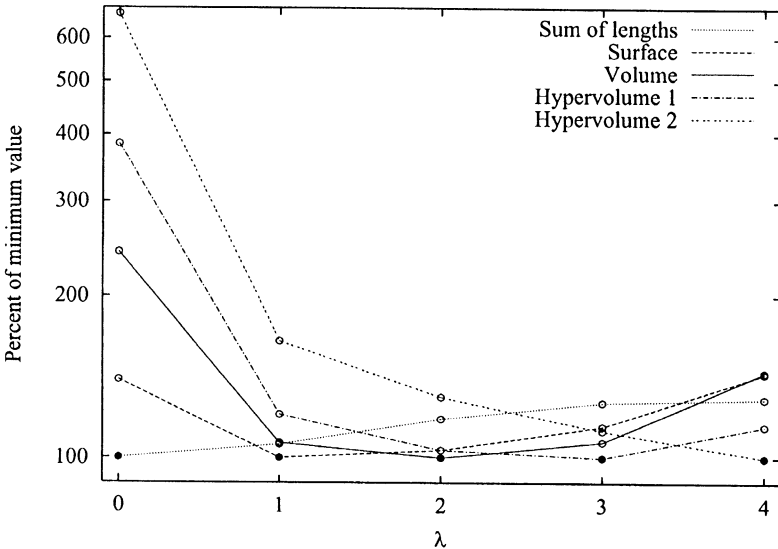


Figure 2: Relative magnitude of various global quantities of CCO trees, normalized by the value of that quantity when it is minimized (i.e., used as target function, filled circles). Target functions are characterized by the parameter  $\lambda$  in Eq. (2). Hypervolume 1 and 2 corresponds to  $\lambda = 3$  and 4, respectively.

## 42 Simulations in Biomedicine IV

Interestingly, a CCO tree with  $\lambda = 0$ , i.e., minimum sum of segment lengths, appears to be heavily suboptimal with regard to total surface, volume, and hypervolumes (up to 660 %), whereas the sum of segment lengths itself seems to be a rather insensitive parameter for discriminating differences in tree structure (only 30 % increase for  $\lambda = 4$ ; dotted line in Fig. 2). Considering the striking visual differences between trees with  $\lambda = 0$  and  $\lambda > 0$  in Fig. 1, this might appear quite unexpected, but can be explained by our particular choice of target function. At  $\lambda = 0$ , the object is to minimize the total sum of segment lengths, regardless of radii, and the length of “small” (i.e., small in radius) segments contributes to the sum with the same weight as the length of “large” ones. Since there is almost no target function penalty for detours as long as they do not involve a large number of segments, it is still rewarding for CCO to allow for some detours of the (relatively few) large vessels, while the majority of small segments is kept short. With  $\lambda > 0$ , however, segment radii become increasingly important in the sense that segment lengths are weighted by their radius, cross-sectional area, etc. Now the length of a large segment enters with higher weight than the length of a small one, and CCO has to be more restrictive in creating detours of major vessels. Visually, conspicuous detours with  $\lambda = 0$  are suppressed and gradually replaced by more and more straight paths.

Table 1: Quantitative effect of target parameter variation on length and shape of a vessel leading to a specific perfusion site in the CCO trees of Fig. 1 (except  $\lambda = 4$ , not shown).

$\lambda$	$n_{\text{bif}}$	$L_{\text{path}}$ [cm]	$L_{\text{bee-line}}$ [cm]	$R_L$
0	139	25.195	6.841	3.683
1	77	10.270	6.932	1.481
2	76	8.067	6.889	1.171
3	58	7.356	7.009	1.049
4	45	7.045	6.888	1.023

So far, we have explained why it is reasonable to expect structural differences between CCO trees generated with different values of  $\lambda$ , and we have commented on their visual appearance. Next, we will investigate some numerical indices which could be used to quantify and evaluate these differences. First, Table 1 demonstrates the influence of the target function parameter  $\lambda$  on the length and shape of a vessel whose terminal segment delivers blood at a selected (but arbitrary) position of the perfusion area (this is the vessel colored dark in Fig. 1). While the length of the bee-line ( $L_{\text{bee-line}}$ ) is approximately constant for all trees, the length of the vessel ( $L_{\text{path}}$ ) and the path-to-bee-line ratio ( $R_L$ ) decrease significantly when  $\lambda$  is

increased from 0 to 4, and the shape of the vessel changes from a meandering structure through more and more streamlined paths to fully straightened tubes. At the same time the number of bifurcation levels shrinks from 139 to only 45.

Figure 3 shows the influence of the target function on blood transport path length in a series of CCO trees with  $\lambda$  varying from 0 to 2 in steps of 0.2 as well as for  $\lambda = 3$  and 4. The path-to-bee-line ratio  $R_L$  has been averaged over all terminal segments of a tree to yield a global characteristic for the tree structure. Minimum and maximum values as well as standard deviations indicate the range of variability. With increasing values of  $\lambda$  a monotonous decrease of  $R_L$  can be observed: While for  $\lambda = 0$  the path length from the root to the terminal segment is—in consequence of numerous detours through the strongly curved vessels—on the average 2.3 times longer than the bee-line, the extent of detours is only 1.04 for  $\lambda = 4$ .

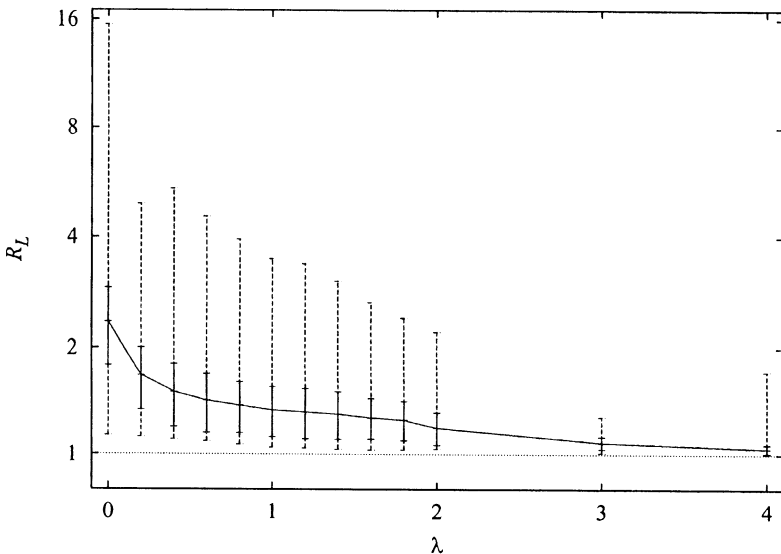


Figure 3: Path-to-bee-line ratio of CCO trees with different values of the optimization target function parameter  $\lambda$ . The solid line joins mean values (averaged over all terminal segments of a tree). Standard deviations, minima and maxima are shown by solid and dashed bars, respectively.

So far, only terminal segments have been considered, but straight lines from the root segment can, of course, be calculated for *all* segments in a tree. Figure 4 shows the distribution of segment orientations, i.e. the angle between the direction of a segment and the straight line from the root to the segment's distal end. This is another way of characterizing the “directness”

## 44 Simulations in Biomedicine IV

with which blood is transported to the perfusion sites. In a CCO tree with  $\lambda = 4$ , where large vessels are almost straight tubes and blood access is very direct, the number of parallel oriented segments (small angles) is comparatively high, whereas antiparallel orientated segments (large angles) rarely appear. In contrast, for  $\lambda = 0$  and highly meandering vessels, segments are almost randomly oriented, and for the remaining trees the distributions fall in between.

Visual inspection of the trees suggests that there might be a correlation between radii of vessel segments and their orientation: Large segments mostly seem to “come from the root”. In other words, small angles are expected to occur much more often with large segments than with small ones. Fig. 5 demonstrates this quantitatively: The median values show that for all trees the orientation angles of segments with  $r \geq 0.5\text{mm}$  are on the average much smaller than of segments with  $r < 0.5\text{mm}$ . A comparison between trees shows that the medians steadily decrease as  $\lambda$  increases from 0 to 4. While angles of small vessels may assume maxima of  $180^\circ$  in all trees (not shown), the maximum angles of large vessels drastically decrease for  $\lambda = 0, 1, \dots, 4$ .

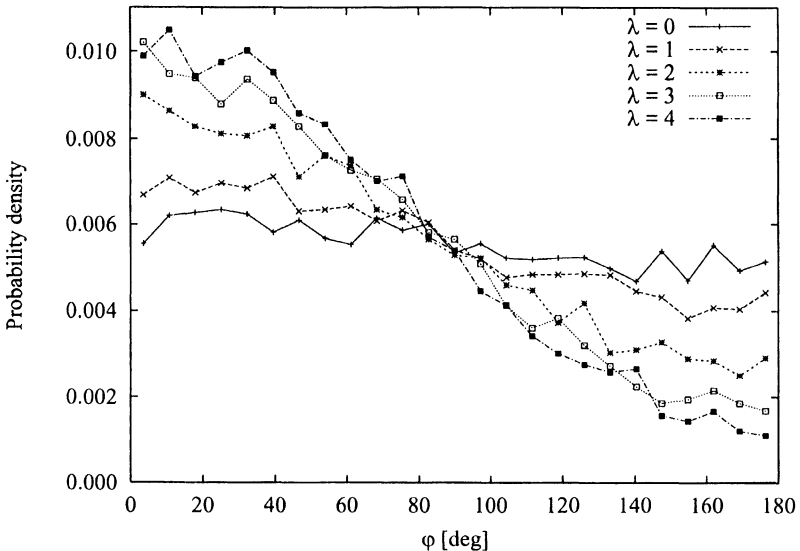


Figure 4: Segment orientation in CCO trees with different values of the optimization target function parameter  $\lambda$ .  $\varphi = 0$  indicates parallel,  $\varphi = 180$  antiparallel orientation of a segment with respect to a straight line from the root segment (proximal end) to the respective perfusion site.



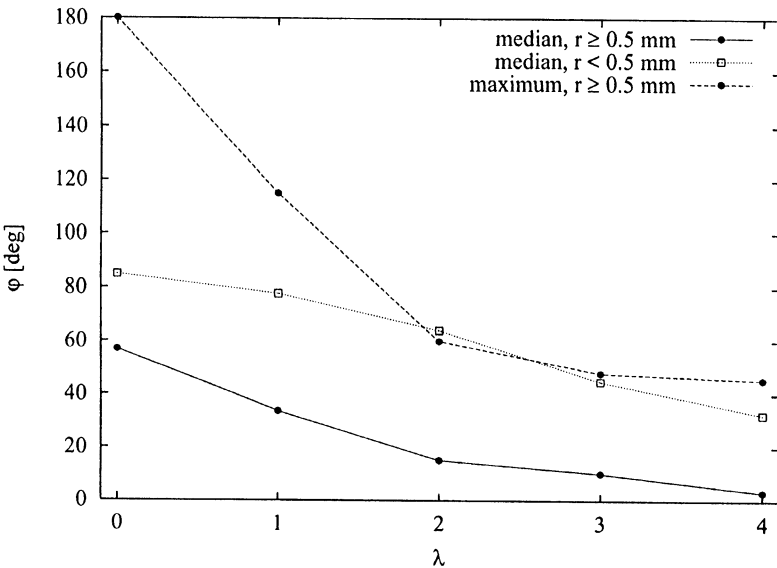


Figure 5: Median and maximum values of segment orientation  $\varphi$  (i.e., the angle between a segment and a straight line from the root) in trees with different values of the optimization target function parameter  $\lambda$ . Segments are classified according to their radius (see legend).

### 3 Conclusion

Summarizing the major results of the study, we could show that global characteristics of CCO trees generally react in a smooth rather than in a discontinuous way to gradual changes of the target function parameter ( $\lambda$ ), and why an increase of  $\lambda$  changes structure from twisted to straight. Furthermore, numerical indices were defined to illustrate different aspects of the same phenomenon (zig-zag versus straight course of vessels): While the path-to-bee-line ratio could discriminate between trees for  $\lambda < 2$ , but was surprisingly low and almost constant for  $\lambda \geq 2$ , segment orientation was found to discriminate satisfactorily over the whole range of  $\lambda$ .

Finally it should be mentioned that our choice of target function is arbitrary, and one might as well think of using other physiologically meaningful functional parameters such as, for instance, shear stress (e.g. Zamir [7]). In that case, the restriction by the bifurcation law [Eq. (1)] would have to be abandoned in favor of another suitable constraint. Also, instead of equal flows and pressures at all terminal segments, one could require equality of terminal radii. In all such instances the effect of parameter variation of the target function on the structure of the trees might be qualitatively and quantitatively different from the present case.



## 46 Simulations in Biomedicine IV

**Acknowledgement.** This work was supported by the Bundesministerium für Wissenschaft und Forschung, grant no. 49.820/4-24/92.

## References

1. Thompson, D.W. *On growth and form*, Dover, Mineola, N.Y., 1992 (reprint of the 2nd edition, Cambridge, 1942), pp. 948–957.
2. Kamiya, A. & Togawa, T. Optimal branching structure of the vascular tree, *Bulletin of Mathematical Biophysics*, 1972, **34**, 431–438.
3. Schreiner, W. & Buxbaum, P. Computer-optimization of vascular trees, *IEEE Transactions of Biomedical Engineering*, 1993, **40**, 482–491.
4. Schreiner, W., Neumann, F., Neumann, M., End, A., Rödler, S.M. & Aharinejad, S. The influence of optimization target selection on the structure of arterial tree models generated by constrained constructive optimization, *Journal of General Physiology*, 1995, **106**, 583–599.
5. Rodbard, S. Vascular caliber, *Cardiology*, 1975, **60**, 4–49.
6. Sherman, T.F. On connecting large vessels to small: the meaning of Murray's law, *Journal of General Physiology*, 1981, **78**, 431–453.
7. Zamir, M. Shear forces and blood vessel radii in the cardiovascular system, *Journal of General Physiology*, 1977, **69**, 449–461.